


Article

# A Multi-Position Drum-Type Assembly for Simultaneous Film Deposition at Different Temperatures in a Single Sputter Cycle—Application to ITO Thin Films

Akhmed K. Akhmedov <sup>1</sup>, Abil S. Asvarov <sup>1,2,\*</sup> , Arsen E. Muslimov <sup>2</sup>  
and Vladimir M. Kanevsky <sup>2</sup>

<sup>1</sup> Institute of Physics, Dagestan Research Center of Russian Academy Sciences, Yaragskogo str., 94, 367015 Makhachkala, Russia; cht-if-ran@mail.ru

<sup>2</sup> Shubnikov Institute of Crystallography, Federal Scientific Research Center “Crystallography and Photonics” of Russian Academy of Sciences, Leninsky Prospect, 59, 119333 Moscow, Russia; amuslimov@mail.ru (A.E.M.); kanev@crys.ras.ru (V.M.K.)

\* Correspondence: abil-as@list.ru

Received: 8 October 2020; Accepted: 5 November 2020; Published: 9 November 2020



**Abstract:** The design of a multi-position drum-type assembly (MPDTA) for heating and positioning substrates with the possibility of individually setting and controlling the temperature of each substrate, which is applicable for laboratory-type sputtering setups, is described. The above design provides the possibility of the simultaneous deposition of thin films under identical conditions on several substrates at different temperatures, making it possible to explore the temperature dependences of the films’ morphology, structure, and functional characteristics in one single vacuum deposition cycle. As a case study, the possibility of investigating such dependencies for the magnetron deposition of transparent conducting indium–tin oxide (ITO) thin films was demonstrated using the MPDTA. The investigation results revealed that the functional performances of deposited ITO thin films (resistivity and average transmittance in the visible range) improved with increasing the substrate temperature, reaching values of  $1.5 \times 10^{-4} \Omega\text{-cm}$  and over 80%, respectively, at 300 °C.

**Keywords:** substrate holder; heating; magnetron sputtering; thin film; ITO; transparent conductive oxide

## 1. Introduction

A heated substrate holder represents a fundamental component of any sputtering setup. Typically, its design is determined by the range of tasks implemented on the basis of a particular sputtering setup. For example, setups designed for the physical vapor deposition (PVD) of films on a plurality of relatively small substrates are equipped with a drum or planetary-type holder that allows each of the substrates to pass sequentially and repeatedly in front of the target [1]. In such setups, the heating of substrates is performed by IR radiation from an external stationary heater [2]. This holder concept provides the same temperature regime for all substrates and is widely used in both industrial and semi-industrial sputtering setups, with the aim of depositing functional thin films according to an already well-established route. Indirectly heated substrate holders are commonly used in most laboratory PVD setups for routine explorations. At the same time, the use for research purposes of a setup featuring a multi-position substrates holder with the possibility to set individually the temperature for each substrate would provide simultaneous deposition capabilities of thin films under identical technological conditions on several substrates at different temperatures in the same vacuum cycle [3–5]. This will make it possible to obtain promptly complete information on the substrate

temperature influence over the deposition rate, morphology, structure, and functional characteristics of the deposited thin film materials [6]. In addition to speeding up the optimization of the deposition process, this concept of a multi-position substrate holder with independent heating systems should result in increased reliability of the obtained research results, which is completely in line with the high-throughput paradigm [7].

In this paper, the design of a multi-position drum-type assembly (MPDTA) that provides simultaneous setting and control of the temperature of up to six substrates is presented. Then, the performance and advantages of the developed MPDTA are applied to the deposition of a transparent conductive oxide (TCO) material, ITO, since extensive research in this area (the influence of the growth parameters on the properties and the stability of the TCO films) is still relevant [8–11]. It is noteworthy that the upper limit for the optimization of growth conditions with respect to the substrate temperature for most TCO materials usually does not exceed 500 °C [9,10].

## 2. Materials and Methods

### 2.1. Description of the Developed MPDTA

The functional scheme of the MPDTA designed for the positioning and heating of substrates is shown in Figure 1a. The MPDTA is mounted on the upper lifting flange (1) of the vertical cylindrical working chamber of our sputtering setup. MPDTA consists of a disk faceplate (2), on which, using corner consoles (3), several substrate holders (4) are installed (up to six). Each substrate holder is a stainless steel bar (with a 25 mm × 40 mm–working surface) equipped with a U-shaped spiral heater and a K-type thermocouple. The heaters are electrically insulated from the holder body using quartz tubes. The construction of a coil heater element is shown in Figure S1 of the Supplementary Materials (SM). A hollow shaft (6) is coaxially mounted in the center of the faceplate (2), through which the connecting wires from the heaters and the cold ends of thermocouples (5) are brought out and connected to corresponding inner pins (8) into a specially designed electrical feedthrough (7). Some detailed pictures of the electrical feedthrough are presented in Figure S2 of SM. External pins of the feedthrough system have sliding contacts (9), which are set in connection with a terminal block (10) connected to individual proportional-integral-derivative temperature controllers installed in the control rack.

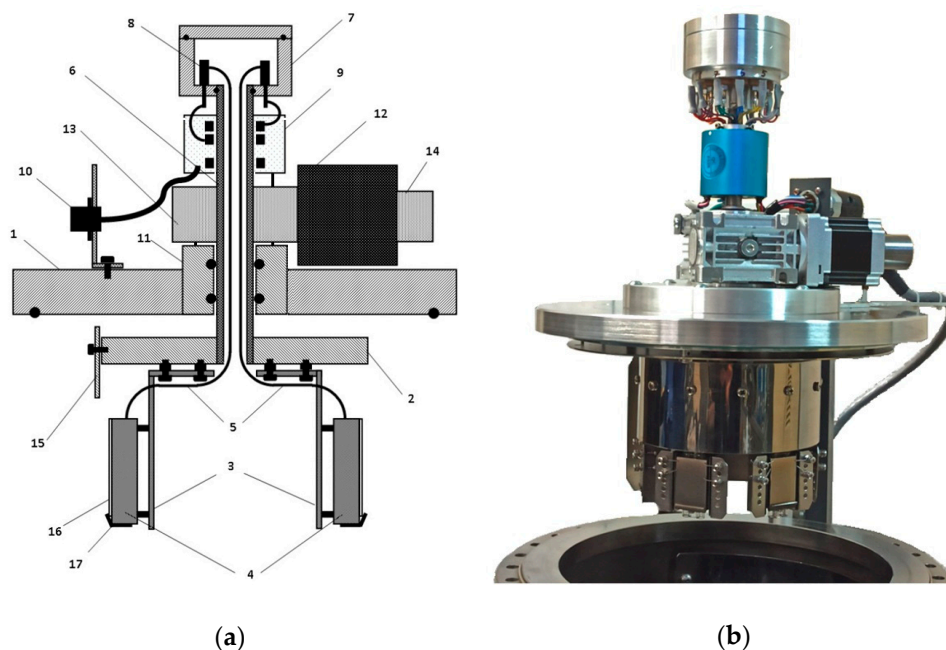


**Figure 1.** (a) Functional scheme of the multi-position drum-type assembly (MPDTA); (b) Appearance of the MPDTA mounted on the upper lifting flange of the sputtering setup.

The hollow shaft (6) is mated with the upper flange (1) through a vacuum rotational joint (11). The vacuum rotary joint is provided by two ceramic bearings and two fluoroelastomeric collars. The disk faceplate (2) is rotated through a worm gear (13) by a stepper motor (12), which is mounted axially on the shaft (6). Additionally, a flywheel (14) is installed on the rear output of the stepper motor shaft, which serves for manual positioning of the substrates. On the faceplate end, a side shield (15) is installed. The clamping of the substrates (16) on the working surface of the holders (4) is carried out using a wedge stop (17) and a number of lateral spring-loaded clamps (Figure S1b in SM).

Figure 1b shows a photograph of the MPDTA containing four independent heated holders and mounted on the sputtering setup featuring a horizontal configuration of magnetron units. The parts 1, 2, 7, 11, and 14 are made of D16T aluminum alloy (analogue of EN AW-2024), and parts 3, 4, 6, 15, and 17 are made of stainless steel 12 × 18H10T (analogue of AISI Type 321). The materials used to create the substrate holder and its construction make it possible to reach the heating of the substrates up to 500 °C. Such an upper limit temperature is suitable to address a number of scientific and technological problems, in particular, for optimizing the deposition of various TCO materials, where the upper limit of the substrate temperature range rarely exceeds 400 °C.

The U-shaped spiral heaters with a cold resistance of 8 Ohm, made of 0.5 mm NiCr wire, were used to heat the holders. The maximum power consumption by each heater is 50 W. The ramp for reaching the temperature mode is set by regulating the power supply voltage in the range between 10 and 20 V. The maximum heating rate in a vacuum is about 50 °C/min. Additionally, preliminary mapping of the temperature field on the surface of the substrate fixed on a heated holder in an Ar atmosphere at the pressures of  $10^{-3}$  Pa and 0.5 Pa in the temperature range 50–400 °C with a step of 20 °C/min were carried out, as well as calibration of the temperature. To achieve this, a glass substrate (CORNING 2947 glass, 40 mm × 25 mm × 1.1 mm) with thin thermocouples soldered to the outer surface of the substrate was used. One thermocouple was located in the center of the substrate, while four others were positioned along the edges at a distance of 3 mm from the edges of the substrate. The study showed that the maximum temperature spread over the substrate surface did not exceed ±3%.

The following steps reduced the heat load on the mounting faceplate (2) and vacuum interfaces: (i) the substrate holders were equipped with spaced stainless steel shields with intermediate ceramic bushings made of zirconium dioxide; (ii) a number of holes were made in the corner bracket (3) to reduce heat transfer, the holder bodies in the projections were placed behind the faceplate (2), and the brackets (3) were installed on the faceplate (2) through heat-insulating bushings 5 mm high; and (iii) the inner walls of the chamber and the lifting top flange, on which the assembly was mounted, were also protected from dust and heat by a system of removable stainless steel shields (15). Due to the relatively low power consumption of the heaters ( $\leq 50$  W) and the system of internal shields, the temperature of the outer walls of the chamber did not exceed 60 °C when all heated holders reached 400 °C during 6 h of operation.

It is also worth noting that the drive system used in the MPDTA provides rotational speed variation in the range from 0.01 to 60 rpm. The presence of a stepper motor in the drive system also makes it possible to implement complex rotation algorithms required in the case of the formation of multilayer thin-film structures by the sequential passage in front of two or more sources.

## 2.2. ITO Thin Films Synthesis by Using of the Developed MPDTA

ITO thin films at various substrate temperatures were deposited by sputtering using a home-made direct current magnetron sputtering system equipped by MPDTA in a single vacuum cycle. The sputtering target used for deposition was an  $\text{In}_2\text{O}_3:\text{SnO}_2$  (90:10 wt.%) ceramic disc (Summit-Tech. Co., Zhubei, Taiwan) with a purity of 99.99% and a diameter of 51 mm.

Thoroughly cleaned glass (30 mm × 25 mm) and silicon (25 mm × 10 mm) pieces were fixed on each of the substrate holders of the MPDTA. The base pressure of the deposition chamber is less than  $2 \times 10^{-4}$  Pa (a turbo molecular pump backed by a rotary pump were used). After reaching the base pressure, the chamber was backfilled to working pressure of 0.15 Pa with a gas mixture of Ar–O<sub>2</sub>

(oxygen content of 3%). Then, for this experiment, four different temperatures were set on the four holders of the MPDTA: 50, 100, 200, and 300 °C. To achieve this, the supply voltage of the heaters of each holder was set individually to the minimum required for the synchronous achievement of the set temperature value (therefore, the power consumption for each heater did not exceed 30 W). In this case, the duration of the temperature stabilization of the holders was within 20 min. After stabilization of the set temperature values on each of the holders, a standard power ramp procedure for ITO ceramic target and its pre-sputtering for 10 min on a closed shutter were performed. Then, the shutter of the magnetron was opened, and the rotation of the drum with substrates heated to different temperatures was enabled at the rotational speed of 10 rpm. The deposition was done using DC power supply, which was kept constant at 85 W power. The total time of the sputtering process was 180 min, during which each of the holders with substrates that was heated to 50, 100, 200, and 300 °C passed 1800 times in front of the sputtered target at a distance of 100 mm.

### 2.3. Film Characterization

The crystalline structure and phase of the ITO films deposited at various substrate temperatures on glass substrates were measured using a X-ray diffractometer (XRD, X'PERT PRO MPD, Malvern Panalytical Ltd., Malvern, UK) with a CuK $\alpha$  source ( $\lambda = 1.5418 \text{ \AA}$ ) at a power of 40 kV/30 mA. The morphology of the ITO thin films on Si substrates was studied by scanning electron microscopy (SEM, Leo-1450, Carl Zeiss, Oberkochen, Germany). Film thicknesses were measured using cross-sectional SEM images.

The sheet resistance of the ITO thin films was measured using a four-point technique (IUS-3, Moscow, Russia). The optical transmittance of the ITO thin films coated on glass substrates was recorded by an optical spectrophotometer (Shimadzu UV-3600, Tokyo, Japan).

## 3. Results and Discussion

In this section, we briefly justify the performance of our MPDTA apparatus in presenting the characterization results related to the microstructure and functional performances of transparent conducting ITO films deposited at different temperatures in the same batch.

### 3.1. SEM Analysis

Cross-section and surface morphology micrographs of the ITO thin films are shown in Figure 2. Data from cross-sectional images allowed us to measure film thickness  $h$  (Figure 2a).  $h$  is the same for all the samples,  $410 \pm 5 \text{ nm}$ , and there is not any dependence of  $h$  on the substrate temperature. This first result confirms the quality of the setup.

The thin films all have a columnar structure characteristic of ion-plasma growth methods [12], and the transverse size of the columns increases with increasing temperature [13].

Looking at Figure 2b, we can observe a smooth growth pattern of the ITO film grown at a substrate temperature of 50 °C, featuring a dense morphology. At higher substrate temperatures, the granular microstructure becomes visible.

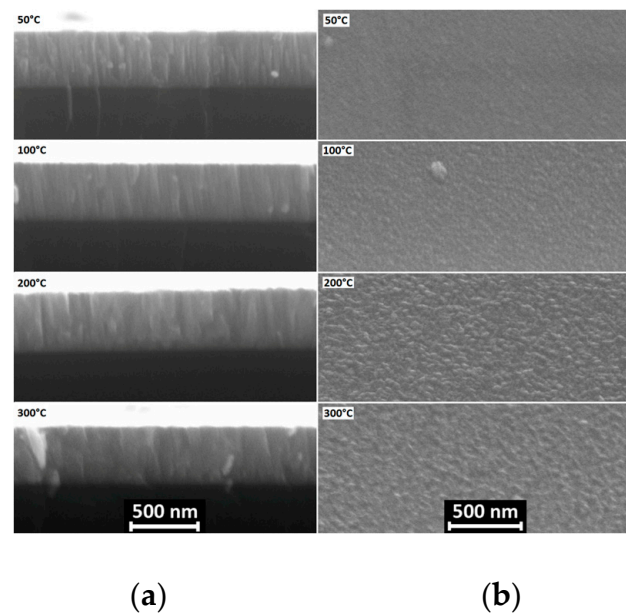


**Figure 2.** (a) Cross-section morphologies of the indium–tin oxide (ITO) thin films; (b) Surface morphologies of the ITO thin films. Substrate temperature shown in the insets.

### 3.2. XRD Analysis

Figure 3a shows the XRD spectrum of the ITO sputtering target. It shows pretty well the crystalline structure, with diffraction peaks corresponding to (211), (222), (400), (440), (622), and other crystalline planes, that match with  $\text{In}_2\text{O}_3$  reference peaks in the body-centered cubic (bcc) polytype. The observed intensities of diffraction peaks are close to the intensities of the lines in the reference spectrum of  $\text{In}_2\text{O}_3$  (JCPDS # 06-0416), which indicates the absence of any preferred orientation in the ceramic target. The XRD pattern did not show any characteristic peak of Sn-related phases, indicating the complete miscibility of In and Sn atoms in the  $\text{In}_2\text{O}_3$  lattice for the sintered ITO ceramic target.

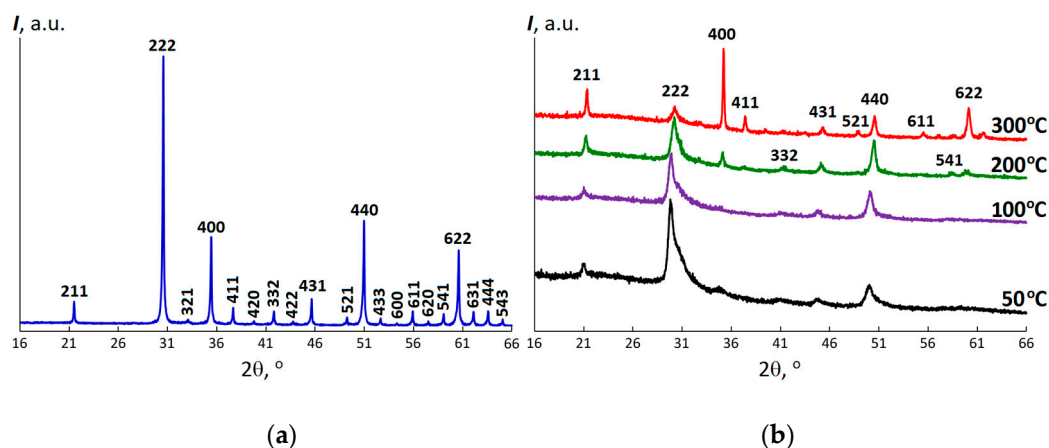


**Figure 3.** (a) XRD pattern of the ITO ceramic target source; (b) XRD patterns of the ITO thin films deposited at various substrate temperatures. All peaks and temperatures have been labeled.

A quite different picture emerges from the analyses of the thin ITO films (Figure 3b). The XRD patterns show that the nanocrystalline phase can be best described by the bcc  $\text{In}_2\text{O}_3$  structure too, but in the films, there are various preferred crystallographic orientations, which are this time influenced by the substrate temperature. It is clear that the structure and orientation of ITO film deposited at a 50 °C substrate temperature exhibits a dominant asymmetric (222) peak. By increasing the substrate temperature, an increase in the intensity of (211), (400), (410), (440), and (622) peaks, accompanied by

the suppression of the asymmetric (222) peak, is observed. In the substrate temperature range between 100 and 200 °C, the ITO films increasingly develop the (440) preferred orientation, while the ITO film deposited at the substrate temperature of 300 °C already has a strong (400) preferred orientation. For the ITO films prepared by sputtering, changes in the preferred orientations from (222) to (400) have been reported by several groups with increasing sputtering power [12,14], decreasing oxygen partial pressure [15] as well as with increasing substrate temperature [16]. These parameters enhance the surface mobility of adatoms and increase the number of oxygen vacancies that favors the film growth along some lower-index crystallographic planes.

It should also be noted that the presence of the (222) highly asymmetry peak, which is clearly observed for the films deposited at temperatures below 300 °C, suggests the presence of two subpopulations of nanocrystallites (both with normal and with higher Sn content) in the In-Sn-O ternary system with different crystallinity degrees [17,18].

With an increase in the substrate temperature (especially above 100 °C), along with the suppression of the (222) peak and the disappearance of its asymmetry, a decrease in integral width and a peak shift toward the position of the lines of the reference  $\text{In}_2\text{O}_3$  are observed for all peaks, which is a finding that was expected. This behavior is evidence of a decrease in the lattice disordering in Sn-doped  $\text{In}_2\text{O}_3$  nanocrystallites due to the thermodiffusion of Sn atoms from interstitial locations and grain boundaries into the In cation sites, as well as an increase in the average crystalline size with increasing substrate temperature [12,19].

### 3.3. Functional Performances

The improvement in the crystallinity of the ITO films upon increasing the substrate temperature is directly reflected in the main functional performances of ITO—namely optical transmittance and electrical conductivity.

The optical transmission spectra for ITO films in the wavelength range between 300 and 1250 nm are shown in Figure 4. It is seen that all films are characterized by a high optical transparency (>84%) in the visible range, regardless of substrate temperature. The measured average transmittances  $T_{av}$  for the ITO/glass structure falls in the range of 380–760 nm, and these are presented in Table 1. According to Table 1, the total average transmittance of the ITO/glass structure (ITO/glass) tends to increase from 76.0% to 80.4% with increasing substrate temperature.

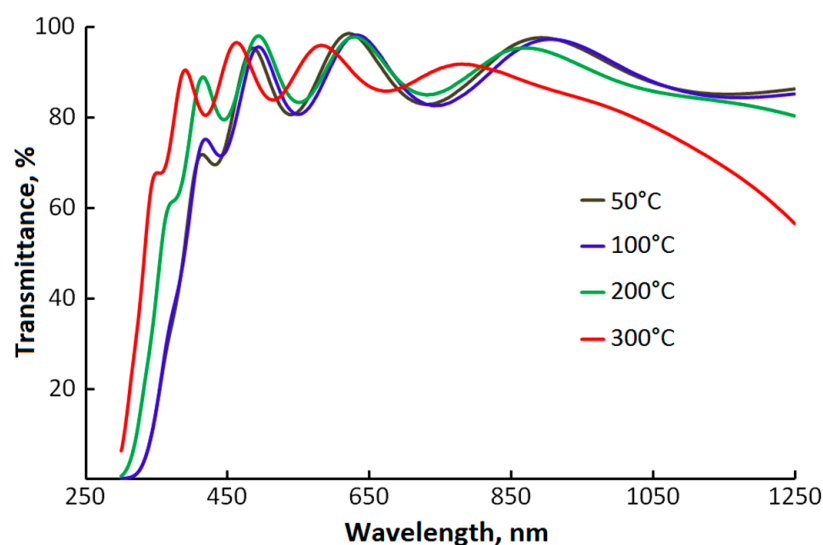


**Figure 4.** Transmittance spectra in the 300–1250 nm region for ITO thin films deposited at various substrate temperatures (glass substrate contribution subtracted).

**Table 1.** Measured sheet resistance  $R_{\square}$ , calculated film resistivity  $\rho = R_{\square} \times h$ , average transmittances  $T_{av}$  in the range of 380–760 nm, and figure of merit  $\phi = (T_{av})^{10}/R_{\square}$  of the ITO glass.

$T_{sub}, ^\circ\text{C}$	$R_{\square}, \Omega/\text{sq.}$	$\rho, \times 10^{-4} \Omega\cdot\text{cm}$	$T_{av}, \%$	$\phi, \times 10^{-3} \text{ Ohm}^{-1}$
50	$50.0 \pm 0.5$	$20.9 \pm 0.4$	76.0	1.25
100	$42.0 \pm 0.5$	$17.2 \pm 0.4$	75.9	1.49
200	$8.3 \pm 0.1$	$3.4 \pm 0.08$	79.6	12.2
300	$3.6 \pm 0.1$	$1.5 \pm 0.04$	80.4	30.5

The observed fluctuations in the spectra are connected with the interference of light, which is due to the quality features and smoothness of the ITO films' interfaces. The differences in the interference pattern for the ITO films with the same thickness should testify to the variation of optical features (optical band gap, dispersions of refractive index, and extinction coefficient) of the nanostructured thin films, which are usually correlated directly with their microstructure and morphology [20]. It can be seen that ITO films deposited at 50 and 100 °C are characterized by almost identical optical transmission spectra. Increasing the substrate temperature above 100 °C leads to noticeable changes in the interference pattern and shifting of the fundamental absorption edge, which indicates the shift of the band gap of the ITO films. In accordance to our SEM and XRD data, noticeable changes in the morphology and microstructure were also observed with an increase of the substrate temperature to 200 °C and above.

Both the observed shift of the absorption edge in the ultraviolet region as well as the decrease in transparency in the near infrared region might be associated with an increase in the concentration of free charge carriers in the transparent ITO films [12,15,21,22]. This fact, as well as the observed improvement in the crystallinity of the films, which entails a decrease in the scattering of charge carriers, should naturally lead to a significant improvement in the electrical properties of the films [10,12,19]. Indeed, according to Table 1, which shows the main functional performances, the sheet resistance  $R_{\square}$  rapidly decreases with an increase of the substrate temperature up to 200 °C. The film deposited at 300 °C exhibits the lowest resistance of 3.6  $\Omega/\text{sq.}$  and, accordingly, the lowest resistivity of  $1.5 \times 10^{-4} \Omega\cdot\text{cm}$ . The quality index proposed by Haake [23] for measuring the performance of our ITO glass is of  $30.5 \times 10^{-3} \text{ Ohm}^{-1}$ . This value is typical for commercial samples of conductive glass [24,25], matches with the best values from literature data on ITO-based transparent electrodes [14,19,26], and fully validates the MPDTA assembly as a useful tool for both scientific research and industrial production.

#### 4. Conclusions

In order to quickly optimize the film growth temperature in physical vapor deposition, we have developed the multi-position drum-type assembly (MPDTA) for the simultaneous growth of films on substrates at different controlled temperatures in a single vacuum run. The MPDTA allows depositing thin films on several substrates (up to 6), whose temperature can be independently fixed in the range between room temperature and 500 °C. To validate the assembly, we grew films of the extensively studied Sn-doped  $\text{In}_2\text{O}_3$  material, in a single run, using the MPDTA. The optimization of transparent conducting film growth temperature was demonstrated. Variations in functional performances of deposited ITO thin films were clearly observed as a function of substrate temperature, and these performances are directly related to the different morphologies and nanocrystalline structures of the films. At 300 °C, the Haake quality index of the ITO glass was  $30.5 \times 10^{-3} \text{ Ohm}^{-1}$ , therefore matching the best known values.

In conclusion, the main achievements of using the MPDTA are (i) the capability to optimize growth temperatures in a single vacuum run and (ii) the identical technological conditions submitted to all samples with the exclusion of influences from random factors, which fully meet the high-throughput paradigm.

**Supplementary Materials:** The following are available online at <http://www.mdpi.com/2079-6412/10/11/1076/s1>, Figure S1: Photos of one of the heated holders of the MPDTA seen from different angles, Figure S2: Additional information about the vacuum electrical connector.

**Author Contributions:** A.K.A. designed and made the assembly. A.K.A. and A.S.A. carried out most of the deposition experiments. A.E.M. and A.S.A. performed the investigations of samples properties. A.S.A. and V.M.K. analyzed the data. Writing—original draft preparation A.K.A. and A.S.A.; writing—review and editing, A.S.A. In this study, V.M.K. provided the financial and technical support for designing and conducting the research, as well as supervised the whole research process. All authors have read and agreed to the published version of the manuscript.

**Funding:** This research was performed in the frame of state assignments of Ministry of Science and Higher Education of the Russian Federation for Dagestan Federal Research Center of Russian Academy of Sciences (Dagestan FRC of RAS) and Federal Scientific Research Center “Crystallography and Photonics” of Russian Academy of Sciences (FSRC “Crystallography and Photonics” RAS) and partially funded by Russian Foundation for Basic Research (research project No. 18-29-12099 (A.E.M.), No. 20-02-373 (V.M.K. and A.S.A.), and No. 20-07-00760 (A.K.A.)).

**Acknowledgments:** The authors are grateful for additional technical support from the Shared Research Centers of Dagestan FRC of RAS and FSRC “Crystallography and Photonics” RAS. Access to the equipment of the Shared Research Center of FSRC “Crystallography and Photonics” RAS was supported by the Ministry of Science and Higher Education of the Russian Federation (project RFMEFI62119×0035). The authors acknowledge Alessandro Chiolerio for useful discussions and good recommendations during performing and preparation of the presented work.

**Conflicts of Interest:** The authors declare no conflict of interest.

## References

1. Akhmedov, A.K.; Abduev, A.K.; Kanevsky, V.M.; Muslimov, A.E.; Asvarov, A.S. Low-temperature fabrication of high-performance and stable GZO/Ag/GZO multilayer structures for transparent electrode applications. *Coatings* **2020**, *10*, 269. [[CrossRef](#)]
2. Swart, P.L.; Lacquet, B.M.; Reynecke, S. A substrate heater with fast response for a low current ion-implanter. *IEEE Trans. Nucl. Sci.* **1993**, *40*, 262. [[CrossRef](#)]
3. Hanak, J.J. The “multiple-sample concept” in materials research: Synthesis, compositional analysis and testing of entire multicomponent systems. *J. Mater. Sci.* **1970**, *5*, 964. [[CrossRef](#)]
4. Han, Y.; Siol, S.; Zhang, Q.; Zakutayev, A. Optoelectronic properties of strontium and barium copper sulfides prepared by combinatorial sputtering. *Chem. Mater.* **2017**, *29*, 8239. [[CrossRef](#)]
5. Fekete, A.; Jakab-Farkas, L. Practical and low-cost solution for the temperature control of a substrate heater for thin film deposition. In Proceedings of the 2018 International Conference on Development and Application Systems (DAS), Suceava, Romania, 24–26 May 2018. [[CrossRef](#)]
6. Ohkubo, I.; Christen, H.M.; Kalinin, S.V.; Jellison, G.E., Jr.; Rouleau, C.M.; Lowndes, D.H. High-throughput growth temperature optimization of ferroelectric  $\text{Sr}_x\text{Ba}_{1-x}\text{Nb}_2\text{O}_6$  epitaxial thin films using a temperature gradient method. *Appl. Phys. Lett.* **2004**, *84*, 1350. [[CrossRef](#)]
7. Gregoire, J.M.; van Dover, R.B.; Jin, J.; DiSalvo, F.J.; Abruña, H.D. Getter sputtering system for high-throughput fabrication of composition spreads. *Rev. Sci. Instrum.* **2007**, *78*, 072212. [[CrossRef](#)]
8. Tran, D.-P.; Lu, H.-I.; Lin, C.-K. Conductive characteristics of indium tin oxide thin film on polymeric substrate under long-term static deformation. *Coatings* **2018**, *8*, 212. [[CrossRef](#)]
9. Deyu, G.K.; Hunka, J.; Roussel, H.; Brötz, J.; Bellet, D.; Klein, A. Electrical properties of low-temperature processed Sn-doped  $\text{In}_2\text{O}_3$  thin films: The role of microstructure and oxygen content and the potential of defect modulation doping. *Materials* **2019**, *12*, 2232. [[CrossRef](#)]
10. López, M.; Frieiro, J.L.; Nuez-Martínez, M.; Pedemonte, M.; Palacio, F.; Teixidor, F. Nanostructure ITO and get more of it. Better performance at lower cost. *Nanomaterials* **2020**, *10*, 1974. [[CrossRef](#)] [[PubMed](#)]
11. Joo, S.Y.; Loka, C.; Jo, Y.W.; Reddyprakash, M.; Moon, S.W.; Choi, Y.; Lee, S.E.; Cho, G.S.; Lee, K.-S. ITO/SiO<sub>2</sub>/ITO structure on a sapphire substrate using the oxidation of ultra-thin si films as an insulating layer for one-glass-solution capacitive touch-screen panels. *Coatings* **2020**, *10*, 134. [[CrossRef](#)]
12. Dong, L.; Zhu, G.; Xu, H.; Jiang, X.; Zhang, X.; Zhao, Y.; Yan, D.; Yuan, L.; Yu, A. Fabrication of nanopillar crystalline ITO thin films with high transmittance and IR reflectance by RF magnetron sputtering. *Materials* **2019**, *12*, 958. [[CrossRef](#)] [[PubMed](#)]



13. Rogozin, A.; Vinnichenko, M.; Shevchenko, N.; Vazquez, L.; Mücklich, A.; Kreissig, U.; Yankov, R.A.; Kolitsch, A.; Möller, W. Effect of elevated substrate temperature on growth, properties, and structure of indium tin oxide films prepared by reactive magnetron sputtering. *J. Mater. Res.* **2007**, *22*, 2319. [CrossRef]
14. Shakiba, M.; Kosarian, A.; Farshidi, E. Effects of processing parameters on crystalline structure and optoelectronic behavior of DC sputtered ITO thin film. *J. Mater. Sci.* **2017**, *28*, 787. [CrossRef]
15. Najwa, S.; Shuhaimi, A.; Talik, N.A.; Ameera, N.; Sobri, M.; Rusop, M. In-situ tuning of Sn doped In<sub>2</sub>O<sub>3</sub> (ITO) films properties by controlling deposition Argon/Oxygen flow. *Appl. Surf. Sci.* **2019**, 479, 1220. [CrossRef]
16. Zhang, W.; Zhu, G.; Zhi, L.; Yang, H.; Yang, Z.; Yu, A.; Xu, H. Structural, electrical and optical properties of indium tin oxide thin films prepared by RF sputtering using different density ceramic targets. *Vacuum* **2012**, *86*, 1045. [CrossRef]
17. Buscaglia, M.T.; Buscaglia, V.; Viviani, M.; Nanni, P.; Hanuskova, M. Influence of foreign ions on the crystal structure of BaTiO<sub>3</sub>. *J. Eur. Ceram.* **2000**, *20*, 1997. [CrossRef]
18. Holder, C.F.; Schaak, R.E. Tutorial on powder X-ray diffraction for characterizing nanoscale materials. *ACS Nano* **2019**, *13*, 7359. [CrossRef]
19. Chen, Y.; Zhou, Y.; Zhang, Q.; Zhu, M.; Liu, F. The correlation between preferred orientation and performance of ITO thin films. *J. Mater. Sci.* **2007**, *18*, S411. [CrossRef]
20. Daza, L.G.; Acosta, M.; Castro-Rodriguez, R.; IRIBARREN, A. Tuning optical properties of ITO films grown by rf sputtering: Effects of oblique angle deposition and thermal annealing. *Trans. Nonferrous Met. Soc. China* **2019**, *29*, 2566. [CrossRef]
21. Thirumoorthi, M.; Thomas Joseph Prakash, J. Structure, optical and electrical properties of indium tin oxide ultra thin films prepared by jet nebulizer spray pyrolysis technique. *J. Asian Ceram. Soc.* **2016**, *4*, 124. [CrossRef]
22. Guillén, C.; Herrero, J. Influence of oxygen in the deposition and annealing atmosphere on the characteristics of ITO thin films prepared by sputtering at room temperature. *Vacuum* **2006**, *80*, 615. [CrossRef]
23. Haacke, G. New figure of merit for transparent conductors. *J. Appl. Phys.* **1976**, *47*, 4086. [CrossRef]
24. BIOTAIN CRYSTAL. Available online: <http://www.crystal-material.com/Substrate-Materials> (accessed on 7 October 2020).
25. KINTEC. Available online: <http://www.kintec.hk> (accessed on 7 October 2020).
26. Yang, S.; Zhong, J.; Sun, B.; Zeng, X.; Luo, W.; Zhao, X.; Shu, Y.; Chen, J.; He, J. Influence of base pressure on property of sputtering deposited ITO film. *J. Mater. Sci.* **2019**, *30*, 13005. [CrossRef]

**Publisher's Note:** MDPI stays neutral with regard to jurisdictional claims in published maps and institutional affiliations.



© 2020 by the authors. Licensee MDPI, Basel, Switzerland. This article is an open access article distributed under the terms and conditions of the Creative Commons Attribution (CC BY) license (<http://creativecommons.org/licenses/by/4.0/>).